



Originally published as:

Bindi, D., Abdrakhmatov, K., Parolai, S., Mucciarelli, M., Grünthal, G., Ischuk, A., Mikhailova, N., Zschau, J. (2012): Seismic hazard assessment in Central Asia: Outcomes from a site approach. - Soil Dynamics and Earthquake Engineering, 37, 84-91

DOI: [10.1016/j.soildyn.2012.01.016](https://doi.org/10.1016/j.soildyn.2012.01.016)

## **Seismic hazard assessment in Central Asia: outcomes from a site approach**

D. Bindi (1,2), K. Abdrakhmatov (3), S. Parolai (4), M. Mucciarelli (5), G. Grünthal (4), A. Ischuk (6), N. Mikhailova (7), J. Zschau (4)

(1) Center for Disaster Management and Risk Reduction Technology, Helmholtz Centre Postdam, GFZ German Research Centre for Geosciences, Potsdam, Germany

(2) Istituto Nazionale di Geofisica e Vulcanologia, Milano, Italy

(3) Institute of Seismology, National Academy of Science, Bishkek, Kyrgyz Republic

(4) Helmholtz Centre Potsdam, GFZ German Research Centre for Geosciences, Potsdam, Germany

(5) Department of Structures, Geotechnics, Engineering Geology -DISGG, University of Basilicata, Potenza, Italy

(6) Institute of Geology, Earthquake Engineering and Seismology, Academy of Sciences of the Republic of Tajikistan, Dushanbe, Tajikistan

(7) Institute of Geophysical Researches of the National Nuclear Center of the Republic of Kazakhstan, Almaty, Kazakhstan

### **Abstract**

In the process of updating existing PSHA maps in Central Asia, a first step is the evaluation of the seismic hazard in terms of macroseismic intensity by applying a data driven method. Following the Site Approach to Seismic Hazard Assessment (SASHA) (D'Amico and Albarello, 2008), the evaluation of the probability of exceedance of any given intensity value over a fixed exposure time, is mainly based on the seismic histories available at different locations without requiring any a-priori assumption about seismic zonation. The effects of earthquakes non included in the seismic history can be accounted by propagating the epicentral information through a Intensity Prediction Equation developed for the analyzed area. In order to comply with existing building codes in the region that use macroseismic intensity instead of PGA, we evaluated the seismic hazard at 2911 localities using a macroseismic catalogue composed by 5322 intensity data points relevant to 75 earthquakes in the magnitude range 4.6-8.3. The results show that for most of the investigated area the intensity having a probability of at least 10% to be exceeded in 50 years is VIII. The intensity rises to IX for some area struck by strong earthquakes in the past, like the Chou-Kemin-Chilik fault zone in northern Tien-Shan, between Kyrgyzstan and Kazakhstan, or in Gissar range between Tajikistan and Uzbekistan. These values are about one degree less than those evaluated in the Global Seismic Hazard Assessment Program (GSHAP; Ulomov, 1999). Moreover, hazard curves have been extracted for the main towns of Central Asia and the results compared with the estimates previously obtained. A good agreement has been found for Bishkek (Kyrgyzstan) and Dushanbe (Tajikistan), while a lower probability of occurrence of I=VIII has been obtained for Tashkent (Uzbekistan) and a larger one for I=IX in Almaty (Kazakhstan).

## Introduction

Central Asia is recognized as one of the most hazardous region in the world and the first attempt to construct a seismic zoning map, where the expected surface shaking is expressed in terms of isoseimal lines for different intensities date back to 1933 (Mushketov, 1933; Savarensky, 1968). In 1978, a general seismic zoning (GSZ) map was released for the former Soviet Union territory (Bune and Gorshkov, 1980), including both boundaries of shaking intensities with zones for intensities from VI to IX of MSK64 scale (Medvedev et al. 1964) and zones of most probable locations of severe earthquakes, differentiated by the maximum expected magnitude, ranging from 6.1 to 8.1. The probability of occurrence was included in an approximate way, in terms of an event occurring once in 100, 1000, and 10000 years, following the recurrence times estimated with the method of Riznichenko (1966) and considering the historical catalogue. In the former Soviet Union, the GSZ maps were also accompanied by seismic zoning map at different spatial scale, like the detailed seismic zoning (DSZ) and the seismic micro zoning (SMZ) maps, characterized not only by different spatial scale, but also by taking into account local seismotectonic, seismic, ground and other natural conditions along with regional ones. In particular, in the SMZ constructed for the main towns, the influence of local site amplifications was also accounted for introducing intensity increments related to local geological conditions.

After the collapse of the Soviet Union, several studies improved the probabilistic hazard assessment in Central Asia. Between 1991 and 1997, a new general seismic zoning (GFZ-97) of Northern Eurasia was realized (Ulomov, 1999) and included as contribution to the Global Seismic Hazard Assessment Program (GSHAP; Giardini, 1999). With regard to this last study, it is important to note that the probabilistic hazard for Central Asia was estimated in terms of intensity and then converted to peak ground acceleration (PGA) by Ulomov (1999) using the Aptikaev and Shebalin (1988) relationship. During the 1990's, the seismic hazard in term of intensities was assessed for many capitals in Central Asia following a probabilistic approach and some results are summarized in Nurmagambetov et al. (1999). As an example, the DSZ map in terms of both intensity and peak ground acceleration was constructed for the suburbs of Almaty (Kyurskeyev, 1993) and the probabilistic values of seismic hazard in Almaty were assessed in terms of peak accelerations and intensity following the Cornell (1968) approach (Mikhailova, 1996). More recently, a new probabilistic seismic hazard assessment in terms of PGA and Arias intensity has been performed at regional scale for Kyrgyzstan (Abdrakhmatov et al., 2003). At a local scale, new probabilistic assessments for Tashkent (Uzbekistan) and Bishkek (Kyrgyzstan) have been computed by Erdik et al (2005). Finally, within the Central Asia Risk Initiative project (CASRI, <http://www.casri.org>) the catalogues needed for improving the hazard assessment in Central Asia have been revised while the seismic microzonation for some capitals were promoted within the projects Central Asian Cross-border Natural Disaster Prevention (CASCADE) and Earthquake Model Central Asia (EMCA) (<http://www.emca-gem.org>) in order to update the DSZ developed during the Soviet time.

At present, the standard building codes for the area require for anti-seismic design the use of macroseismic intensity as input data, and a passage to a PGA driven code is not yet

foreseen. This is why we produced PSHA maps in terms of intensity taking advantage of revised catalogues and new methodologies, in order to provide a step toward a more reliable and updated seismic input for the region that can be used by local practitioners. In this work, we exploit the macroseismic and the parametric catalogues compiled in CASRI to evaluate the probabilistic seismic hazard in central Asia. The availability of a common catalogues for different countries allows us to perform a cross-border hazard assessment following a homogeneous approach. In particular, the seismic hazard from intensity data is computed using the site approach proposed by Magri et al (1994) and later developed by Albarello and Mucciarelli (2002) and D'Amico and Albarello (2008). Following the site approach, the hazard is computed considering only the seismic history at each site. Then, if in one hand the hazard could be underestimated when the historical catalog is lacking of significant large earthquakes that might occur, on the other hand the hazard is assessed without any a-priori assumption on seismic zonation or on the model of time recurrence. Therefore, the estimates obtained in this study can be later used to validate the results achieved following standard approaches based on seismic source zones.

## **Method**

The seismic hazard is assessed following an approach entirely based on the seismic histories available at different locations, without requiring any a-priori assumption about source zonation. The hazard is computed site by site and it is expressed as the probability that the considered site is shaken by an intensity greater or equal to the chosen threshold over the assumed exposure time. The method is described in details in D'Amico and Albarello (2008) and implemented in a freeware program available upon request to the authors. We briefly recall that it is based on three steps.

1. In the first step, the local history of seismic effects is build for each site.
2. Then, the completeness of the seismic history is assessed using the statistical procedure developed by Albarello et al. (2001), which is based on the assumptions that a) the seismogenic process is stationary; b) the most recent part of the catalogue is complete; c) the catalogue is statistically representative of the long-term seismogenic process.
3. Finally, the hazard is computed for different possible choices of the complete part of the site catalogue (D'Amico and Albarello, 2008).

The computed hazard is expressed in the form of a set of hazard curves, each representing the probability that effects greater or equal to a given intensity threshold will be observed at the site during the considered exposure time. Regarding the construction of the seismic history at each site, the felt intensities can be integrated with virtual intensities related to earthquakes whose effects were not surveyed at the site. To this aim, an intensity prediction equation (IPE) is applied to the epicentral information (magnitude and location) available through a parametric catalogue. In this study we apply the equations recently derived for central Asia by Bindi et al. (2011b).

The above described methodology has been already adopted as a benchmark for other PSHA estimates (Mucciarelli et al. 2008), as a direct PSHA estimate for cities (Azzaro et al., 1999) or island states (Galea, 2007), and recent development after L'Aquila (Italy, 2009) earthquake suggested also strategies for de-aggregation studies (Pace et al., 2011).

## Data

The macroseismic data set considered in this study to assess the seismic hazard in Central Asia is composed by 5322 intensity data points associated to 75 earthquakes (Figure 1) occurred between 1880 and 2000. The magnitude, expressed accordingly to the  $M_{LH}$  scale (e.g. Khalturin, 1974), ranges from 4.6 to 8.3 and the intensities were surveyed at 2911 localities. The number of data points for each locality varies from 1 (at 921 sites) to 42, including 231 localities with more than ten observations (Figure 2). The spatial distribution of the sites reflects the topography of the analyzed area (Figure 1), with high density of observations along the main valleys (e.g. around the Issyk lake, in the Fergana basin, in the Alai valley and in the Tajik depression) and few points in the mountain areas (e.g. Pamir). The maximum intensity surveyed in each location is shown in the bottom panel of Figure 2. The largest values correspond to the epicentral areas of the large historical earthquakes shown in Figure 1.

The set of felt intensities at each site is completed using virtual intensities (D'Amico and Albarello, 2008). To this aim, the Intensity Prediction Equation developed for Central Asia (Bindi et al., 2011b) using the same macroseismic catalog are applied to the seismic catalog collected within CASRI project and composed by about 8400 earthquakes with hypocentral depth less than 40 km (Figure 3). Except for few earthquakes with magnitude  $<3.5$ , the magnitude range covered by the catalog is from 3.5 to 8.3 (see histogram in Figure 3). Most of the earthquakes with magnitude larger than 7 (green circles) occurred along the northern Tien-Shan (between Kazakhstan and Kyrgyzstan) and the South-Hissar fault zone (Tajikistan). In particular, a sequence of strong earthquakes occurred along the Chou-Kemin-Chilik fault zone including the 1887, M 7.3 Verny earthquake, the 1889, M 8.3 Chilik earthquake, the 1911, M 8.2 Kemin earthquake and 1938, M 6.9 Kemin-Chou earthquake (e.g. Delvaux et al., 2001; Kalmetieva et al., 2009). Other strong earthquakes occurred in the Chatkal-Fergana (north-western Kyrgyzstan) seismic zone (1946, M=7.5 Chatkal earthquake; Kalmetieva et al., 2009); in southern Tien-Shan (e.g. 1949, M=7.6 Khait earthquake) (Evans et al., 2009); in northern Pamir (1974, M=7.4 Markansu earthquake; Jackson et al., 1979; Langston and Dermengian, 1981); along the border between Tajikistan and Uzbekistan, in the South Gissar source zone (1907, M=7.3 Karatog earthquake; Babaev et al., 2005); in the Pamir area (1911, Sarez M=7.4 earthquake; Babaev et al., 2005). Among the most recent ones, the data set includes the Ms=7.3, 1992 Suusamyр earthquake (Mellors et al., 1997; Ghose et al., 1997), occurred in Kyrgyzstan (northern Tien-Shan), in a region located north-east of the Talas-Fergana fault. The seismic catalog is mainly covering the period 1800-2005 but about 70 earthquakes occurred earlier are also included. Figure 4 shows the cumulative number of earthquakes against time, counting separately earthquakes with magnitude smaller and larger than 5.5. The curve for magnitude  $\geq 5.5$  shows an almost regular increase with time starting from 1880 while the trend for  $M < 5.5$  shows three main slope changes. The first two changes (around 1920 and 1960) correspond to periods of significant improvements in the seismic monitoring of Central Asia, with the installation of local networks. The decrease of the rate after 1990 is related to the collapse of the Soviet Union that led to a general worsening of the local network monitoring in Central Asia

due to the lack of financial support for maintaining the stations and updating the networks. The annual rate is summarized by the Gutenberg-Richter distribution shown in the bottom panel of Figure 4. A least square fit considering the model  $y=a+bM$  provided the values  $a=5.61-0.89M$ , being the 95% confidence bounds for parameters  $a$  and  $b$  equal to (5.46, 5.77) and (0.87, 0.92), respectively. Finally, examples of felt histories for four large towns in Central Asia are shown in Figure 5, considering both observed (red) and virtual (black) intensities. The largest intensities are generally associated to observed data points while the virtual data points improve significantly the distribution of intensities smaller than V.

## Results

Figure 6 shows the intensity with a probability of 10% to be exceeded during an exposure time window 50 years long, considering either the felt intensity histories alone (top left) or both felt and virtual intensities (bottom left). Intensities larger than IX are observed in areas where the strongest earthquakes occurred in the past, as for example in the Chilik-Kemin, Chatkal-Fergana and Gissar-Kokshal seismic zones. While the introduction of virtual sources has no effect over the sites showing large expected intensities, it increases the intensity of the background. It is worth noting that the largest increments, up to six units, are obtained for locations characterized by an incomplete site history not exceeding intensity IV, mostly near the edges of the studied area. This is also confirmed by comparing the bottom left panel of Figure 6 with Figure 2 (bottom), where the maximum observed intensities at each considered location are shown. Figure 6 (bottom right) also shows the results from the GSHAP project, in terms of intensities having 10% probability of exceedence in 50 years (Ulomov, 1999). To make the comparison easier, the site approach is applied to a grid of points covering the investigated area with a resolution of 0.1 degree (top right). The seismic history at virtual points not coincident with an actual locations are constructed using both the IDPs and the seismic histories at close sites (within a radius of 5 km) applying a Bayesian approach (Albarelo and Mucciarelli, 2002; D'Amico and Albarelo, 2008). The intensities estimated in this work are generally lower than those in the GSHAP map of about one intensity unit. In particular, for most of the Kyrgyzstan and Tajikistan territory intensities IX and VIII are predicted by GSHAP and this study, respectively. Regarding the areas struck by the strongest earthquakes in the past, intensities X and IX are predicted by the two studies, with a spatial extension in the GSHAP map probably influenced by the adopted seismic zonation, the different attenuation relationship and by some assumptions (e.g. maximum magnitude) on the source properties.

The results obtained in this study considering both the felt and virtual intensities are also shown in Figure 7 as the probabilities for each site to feel one intensity equal to or greater than a given reference intensity over an exposure time of 50 years. The considered intensities  $I_{ref}$  are VII, VIII and IX (from top to bottom). For  $I_{ref} = VII$ , most of the locations in the investigated area are characterized by a probability larger than 0.5. Increasing  $I_{ref}$ , those places struck by earthquakes with magnitude larger than 7 show probability larger than 0.4 when  $I_{ref} = VIII$  is considered, and larger than 0.15 for  $I_{ref} = IX$ .

These high probability values confirm that several areas in Central Asia are characterized by a high seismic hazard.

### **Assessed hazard for the main towns**

Almaty, formerly called Verny from 1855 to 1921, suffered several destructive earthquakes since the beginning of 1800 (Figure 5). The 1887, M 7.3 Verny earthquake shook the town with intensity I=IX, leading to the collapse of almost all the adobe buildings which constituted the majority of the buildings in town. The 1889, M 8.3 Chilic earthquake shook Almaty with intensity VII-VIII and the 1911, M 8.2 Kemin earthquake generated intensity I=VIII, leading to the collapse or inducing severe damages to about 50 % of the building in town. Accordingly with the GSZ-78 zonation, an intensity I=IX was attributed to Almaty, with a recurrence interval of 1000 years. Later refinements evaluated a return period of 468 years for intensity IX. Regarding the Seismo Micro Zonation (SMZ) of the town, which accounts for local site conditions, intensities from VIII (north-west part of Almaty) to X (eastern part) are ascribed to the town, accordingly to the different soil conditions. It is also worth remembering the presences of areas with possible surface faulting. Figure 8 shows the comparison between the hazard curve estimated in this study for an exposure time of 50 years and the values given by Nurmangambetov et al. (1999). In particular, this study returns higher probabilities for I=VIII and IX with respect to Nurmangambetov et al. (1999). The maximum intensity corresponding to a probability of exceedence lower than 10% in 50 years is X, which confirms Almaty as the large town with the highest hazard level in the part of Central Asia investigated in this study.

Bishkek (formerly also Pishpek and Frunze), is the capital of Kyrgyzstan. The largest earthquakes which struck the city were the 1885, M 6.9 Belovodsk earthquake (I=VII-VIII) and the 1889, M 5.8 Pishpek earthquake (I=VI). The GSZ-78 zonation attributes to Bishkek intensity IX with a recurrence interval of 1000 years, later refined to 794 years. (Nurmangambetov et al., 1999). The SMZ zonation of Bishkek ascribes intensities from VIII, in the southern part of town, to intensities larger than IX in the northern part. The variability of local site amplifications in Bishkek has been recently evaluated (Parolai et al. 2010) and its effect on seismic risk assessed (Bindi et al., 2011a), showing that site effects can contribute to intensity increments as large as 2 units in the north part of the town. Figure 8 compares the hazard curves estimated in this study for Bishkek with the values provided by Nurmangambetov et al. (1999). A general good agreement is observed with slightly higher probability estimated in this study for I=VIII and slightly lower for I=IX. The maximum intensity corresponding to a probability of exceedence lower than 10% in 50 years estimated is IX.

Dushanbe, the capital of Tajikistan, was struck in the past by several earthquakes, that generated intensities up to VI in the city (e.g. the 1907, M 7.3 earthquake Karatag, and the 1949, M 7.4 Khait earthquake). The town is located close to two main fault systems. The South-Gissar fault is located few km from the town and the estimated maximum magnitude associated to this fault is 7.5. The second fault is the Ilek-Vaksh fault, about

20-25 km far from Dushanbe, and characterized by  $M_{\max}=6.5$  (Babaev et al., 2005). The GSZ-78 zonation associated I=IX to Dushanbe, with a recurrence interval of 1000 years. The return period for I=IX and I=VIII were refined to 1995 and to 447 (Nurmangambetov et al., 1999), respectively.

The seismic hazard in Dushanbe is related to both shallow local earthquakes and deep focus distant earthquakes. For these reason, two different zoning maps were proposed for the town, one for building with less than 5 stories and the other for taller buildings (Negmatullaev et al., 1999). The first map includes intensity of VIII (in the central part, along the river) and IX, while the second map is mainly characterized by I=IX. It is worth remembering that, due to the geological conditions in Dushanbe, possible subsidence and non linear effects could occur in the town, as observed in the loess soils close to Dushanbe during the  $M=5.5$ , 1989 Gissar earthquake (Babaev et al., 2005).

The hazard curves computed for Dushanbe are shown in Figure 8. With respect to the probabilities estimated in Nurmangambetov et al.(1999), higher probabilities are estimated for I=VII and VIII. The maximum intensity corresponding to a probability of exceedence lower than 10% in 50 years is IX.

Tashkent, the capital of Uzbekistan, was struck in the past by several earthquakes occurred at distances smaller than 40 km and with magnitude between 4.3 and 6.7, generating intensities between VI and VII in the town. In particular, the 1966,  $M=5.1$  Tashkent earthquake had epicenter inside the urban area and generated large damages, with intensities up to VII. The GSZ-78 zonation attributed I= VIII to Tashkent with a recurrence interval of 1000 years. Accordingly to Nurmangambetov et al. (1999), the return period for I=VIII is 76 years. The MSZ for Tashkent ascribed intensity VIII and IX depending on the soil type. The hazard curves for Tashkent are shown in Figure 8. The maximum intensity corresponding to a probability of exceedence lower than 10% in 50 years is IX. For intensity VIII, the probability estimated in this study (0.14) is significantly lower than the value (0.48) indicated by Nurmangambetov et al. (1999).

## **Reliability assessment**

To assess the robustness of the hazard estimates at different sites, we repeat the hazard computations but adding to each time history one further intensity value corresponding to a hypothetic earthquake occurred today. In particular, we carry out the test as follow:

1) we add to each location a hypothetic intensity relevant to a fake earthquake occurring today. We created three modified data sets, corresponding to added intensities equal to VII, VIII, and IX;

2) we compute the hazard for the original data set ( $p_0$ ) and for the modified one ( $p_{\text{new}}$ ) considering as threshold the intensity value equal to the added one. We then compare the two probabilities estimated for each case. The comparison is performed selecting those localities with  $p_0$  of exceeding the selected intensity in a 50 year period greater than 0.05.



Figure 9 shows the difference between the hazard estimates computed for the modified site history and for the original one, normalized to this last. In general, the relative differences are very small (e.g. for I=VII about 90% of points show a relative differences smaller than 10%). This indicated that the available time histories allow to perform robust estimates. The differences are generally positive, that is the hypothetical intensity has been added after an elapsed time from the last observation shorter than the expected return period for that intensity. Then, the occurrence of the added intensity is not probable accordingly to the return period estimated from the catalog (see for example the results close to the epicentral area of 1992 Suusamy earthquake, whose location is shown in Figure 1). More interesting are the negative differences, which indicate a seismic drought longer than the average return period estimated for that intensity from the catalogue. For locations where the difference is negative, the seismic history at the site could be less representative for evaluating the hazard. Figure 9 shows that some positive differences are obtained for intensity VII and VIII, but small in absolute value. The results are summarized in Figure 10, where the cumulative distribution functions (CDF) of the relative difference for the three considered intensities are shown. The asymmetry of the CDFs is due to the fact that shorter inter-event times (IET) are more probable than longer ones even if no Poissonian assumption is made: the strong monotonically decreasing trend of IET combined with the decreasing frequency distribution of intensity is in fact driving the sharp decrease of hazard shown in Figure 8.

## Conclusions

In this study we applied the site approach (Magri et al. 1994; Albarello and Mucciarelli, 2002; D'Amico and Albarello, 2008) to assess the seismic hazard in Central Asia. In this approach the hazard assessment is mainly guided by the observed seismic histories at each considered site without requiring, for example, the introduction of any seismic zonation. The main advantage provided by the present paper is a step toward a more reliable and updated seismic input that can be used by local practitioners in a region where the standard building codes require for anti-seismic design the use of macroseismic intensity as input data. Moreover, in the future the estimated probabilities of exceedance could be used as a robust term of comparison for other methods, like the standard Cornell-Mc Guire approach to PSHA, which require much more information to construct the inputs. For a comparison between the results obtained by applying the site and the Cornell (1968) approaches to the same region, see the works of Mucciarelli et al. (2008) and Gomez-Capera et al. (2010) performed in Italy.

We compared our results with GSHAP ones. This was particularly significant since the map for the area were calculated in terms of macroseismic intensity and just converted in PGA as a last step (Ulomov, 1999). The comparison shows that in the GSHAP map the intensity are larger of about one intensity unit with respect to this study. Moreover, the highest estimated intensities are spread over larger areas probably as consequence of the adopted seismic zonation or the different attenuation relationship.

Regarding the comparison with the hazard estimates in terms of intensity previously performed, the hazard curves estimated in this study are generally in agreement, except for few cases, as the probability of exceedance of I=VIII over 50 years in Tashkent,

which we found significantly lower. Furthermore, the application of a homogeneous approach to cross-border catalogues, and considering an intensity prediction equations developed for the investigated area, allowed to obtain a systematic evaluation of the hazard over the entire analyzed area. Future efforts will be dedicated to evaluate the hazard following standard approaches and to discuss the differences in terms of assumptions made.

### **Acknowledgments**

We thank D. Albarello and V. D'Amico for sharing with us the SASHA computer code. The data used in this study has been collected within the Central Asia Risk Initiative (CASRI) project. This research has been supported by Central Asian Cross-border Natural Disaster Prevention (CASCADE) and Earthquake Model Central Asia (EMCA) projects. We thanks the reviewers for their useful comments that allowed us to improve the clarity of the paper.

### **References**

- Abdrakhmatov, K., H.-B. Havenith, D. Delvaux, D. Jongmans & P. Trefois 2003. Probabilistic PGA and Arias Intensity maps of Kyrgyzstan (Central Asia), *Journal of Seismology* 7, 203–220
- Albarello, D., R. Camassi, and A. Rebez (2001). Detection of space and time heterogeneity in the completeness of a seismic catalog by a statistical approach: an application to the Italian area, *Bull. Seism. Soc Am.*, 91, 1, 694-703
- Albarello, D., and M. Mucciarelli (2002). Seismic hazard estimates using ill-defined macroseismic data at site. *Pure and Applied Geophysics* 159, 1,289–1,304.
- Aptikaev, F.F. and N.V.Shebalin (1988). Specification of correlation between level of macroseismic effect and dynamic parameters of ground movements, researches on seismic danger, *Question of Engineering seismology*, 29, 98-107, (in Russian)
- Azzaro R., M.S. Barbano, A. Moroni, M. Mucciarelli and M. Stucchi (1999) The seismic history of Catania, *Journal of Seismology*, 3, 3, 235-252, DOI: 10.1023/A:1009818313629
- Babaev, A.M, Ischuk A.R., and S.Kh. Negmatullaev (2005). Seismic conditions of the territory of Tajikistan, *Publication of the International University of Tajikistan*, 93 pages.
- Bindi D., Mayfield M., Parolai S., S. Tyagunov, U. T. Begaliev, K. Abdrakhmatov, B. Moldobekov, and J. Zschau (2011a). Towards an improved seismic risk scenario for

Bishkek, Kyrgyz Republic, *Soil Dyn. Earth. Eng.* 31, 521-525  
doi:10.1016/j.soildyn.2010.08.009

Bindi D., Parolai S., A. Oth, K Abdrakhmatov, A. Muraliev, and J. Zschau (2011b). Intensity Prediction Equations for Central Asia, *Geophys. Journ. International*, accepted

Bune V.I. and G.P. Gorshkov, (1980) Seismic zonation of USSR, Bune V.I. and G.P. Gorshkov editors, Moscow: Nauka, 307 p. (in Russian)

Cornell, C.A., (1968). Engineering seismic risk analysis. *Bull. Seismol. Soc. Am.* 58 (5), 1583–1606.

D'Amico, V., and D. Albarello (2008). SASHA: A Computer Program to Assess Seismic Hazard from Intensity Data, *Seismological Research Letters* 79, 5, 663-671

Delvaux, D., Abdrakhmatov, K.E. & A. L. Strom 2001. Landslides and surface breaks of the Ms 8.2 Kemin earthquake, Kyrgyzstan, *Russian Geology and Geophysics, Geologiya i Geofizika* 42, 1167–1177

Erdik, M., Rashidov, E. Safak and A. Turdukulov (2005). Assessment of seismic risk in Tashkent, Uzbekistan and Bishkek, Kyrgyz Republic, *Soil Dynamics and Earthquake Engineering*, 25, 473-486

Evans, S. G., N. J. Roberts, A. Ischuk, K. B. Delaney, G. S. Morozova, O. Tutubalina (2009). Landslides triggered by the 1949 Khait earthquake, Tajikistan, and associated loss of life, *Engineering Geology*, 109, 195-212.

Galea P. (2007) Seismic history of the Maltese islands and considerations on seismic risk., *Ann. Geoph.*, 50, 6, 725-740

Ghose, S., Mellors, R.J., Korjenkov, A.M., Hamburger, M.W., Pavlis, T.L., Pavlis, G.L., Omuraliev, M., Mamyrov, E., and A. R. Muraliev (1997). The MS = 7.3 1992 Suusamy, Kyrgyzstan, earthquake in the Tien Shan: 2. Aftershock focal mechanisms and surface deformation, *Bull. Seism. Soc. Am.* 87, 23 - 38.

Giardini D (1999). The global Seismic Hazard Assessment Program (GSHAP)-1992/1999, *Annali di Geofisica*, 42, 6, 957-974

Gómez Capera, A.A., V. D'Amico, C. Meletti, A. Rovida, and D. Albarello (2010). Seismic hazard assessment in terms of macroseismic intensity in Italy: a critical analysis from the comparison of different computational procedures, *Bull. Seism. Soc. Am.*, 100, 4, 1614–1631

Jackson, J., P. Molnar, H. Patton, and T. Fitch (1979). Seismotectonic aspects of the Markansu Valley, Tadjikistan, earthquake of August 11, 1974, *Journal Geophys. Res.*, 84, 6157-6167

Kalmetieva Z.A., Mikolaichuk A.V., Moldobekov B.D., Meleshko A.V., Jantaev M.M. and A. V. Zubovich (2009). Atlas of earthquakes in Kyrgyzstan, ISBN 978-9967-25-829-7

Khalturin, V.I. (1974). Correlation between expected and observed magnitude estimates, in Magnitude and energy classification of earthquakes, Volumes 1, 2. Moscow (in Russian).

Kyurskeyev A., A. Nurmagambetov, A. Sydykov, N.N. Mikhailova, and V.I. Shatsilov (1993). Detailed seismic zoning of Almaty industrial area, *Novosti nauki Kazakhstana*. Alma-Ata, Issue 1.

Langston C. A., and J. M. Dermengian (1981). Comment on ‘Seismotectonic aspects of the Markansu Valley, Tadjikistan, earthquake of August 11, 1974’ by J. Jackson, P. Molnar, H. Patton, and T. Fitch, *Journal Geophys. Res.*, 86, 1091-1093.

Magri, L., M. Mucciarelli, and D. Albarello 1994. Estimates of site seismicity rates using ill-defined macroseismic data, *Pure Appl. Geophys.* **143**, 618–632

Medvedev, S., W. Sponheuer, and V. Kárník (1964). Neue seismische Skala Intensity scale of earthquakes, 7. Tagung der Europäischen Seismologischen Kommission vom 24.9. bis 30.9.1962. In: Jena, Veröff. Institut für Bodendynamik und Erdbebenforschung in Jena, vol 77. Deutsche Akademie der Wissenschaften zu Berlin, pp 69-7

Mellors, R. J., F. L. Vernon, G. L. Pavlis, G. A. Abers, M. W. Hamburger, S. Ghose, and B. Iliasov (1997). The Ms=7.3 Suusamy, Kyrgyzstan earthquake:1: Constraints on fault geometry and source parameters based on aftershocks and body-wave modeling, *Bull. Seismo. Soc. Amer.*, **87**,11-22.

Mikhailova N.N (1996). Seismic hazard in quantity characteristics of strong ground motions (on the example of Almaty). Doctor dissertation on physics and mathematics.

Mucciarelli M., D. Albarello, and V. D'Amico (2008). Comparison of Probabilistic Seismic Hazard Estimates in Italy. *Bull. Seism. Soc. Am.*, vol. 98, pp. 2652-2664

Mushketov, D.I. (1933). Opyt seysmicheskogo rayonirovaniya S.S.S.R. Tr. Seismol. Inst. Akad. Nauk S.S.S.R., 33, 1-17

Negmatullaev, S., A. Ischuk, Y. Potekhin (1999). Seismic hazard and building vulnerability in Tajikistan, S.A. King, V. I. Khalturin & B. E. Tucker (eds), Kluwer Academic Publishers, Netherlands, 107-125.

Nurmagambetov A., N. Mikhailova, and W. Iwan (1999). Seismic hazard of the Central Asia region, in Seismic hazard and building vulnerability in post-Sovietic Central Asian republics, S.A. King, V. I. Khalturin & B. E. Tucker (eds), Kluwer Academic Publishers, Netherlands, 1-43.

Pace B., D. Albarello, P. Boncio, M. Dolce, P. Galli, P. Messina, L. Peruzza, F. Sabetta, T. Sanò and F. Visini (2011) Predicted ground motion after the L'Aquila 2009 earthquake (Italy, Mw 6.3): input spectra for seismic microzoning, *Bull. Earthq. Eng.*, 9, 1, 199-230, DOI: 10.1007/s10518-010-9238-y

Parolai S, Orunbayev S, Bindi D, Strollo A, Usupayev S, and M. Picozzi (2010). Site effect assessment in Bishkek (Kyrgyzstan) using earthquake and noise recording data. *Bull. Seism. Soc. Am.* 100,6 , 3068-3082, doi:10.1785/0120100044.

Ryznichenko, Y. (1966). Calculation of ground shaking of the surface points caused by earthquakes in adjustment area, *Physics of the Earth*, 5, 2-32.

Savarensky, E. F. (1968). On the prediction of earthquakes. *Tectonophysics* 6, 1 7-27

Ulomov, V.I., The GSHAP Region 7 working group, (1999). Seismic hazard of Northern Eurasia. *Annali di Geofisica* 42, 1023–1038

## Figure captions

Figure 1 Top: Study area. The epicenters of the main earthquakes (red squares and labels) and the main active faults (red lines) are indicated. Bottom: spatial distribution of the epicenters (blue circle with dimension proportional to the magnitude) of 75 earthquakes included in the macroseismic catalogue used in this study. The main towns are indicated as well (stars).

Figure 2 Top Distribution of the locations included in the macroseismic catalogue. The number of felt intensities at each location is displayed according to the gray scale. Bottom: maximum observed intensity at each considered location.

Figure 3 Distribution of the epicenters (black circles with dimension proportional to magnitude) of the earthquakes used to complete the felt histories by using a intensity prediction equation. Green circles indicate earthquake with  $M > 7$ . In the inset, the distribution of the magnitude values is also shown.

Figure 4. Top. Cumulative number of earthquakes with magnitude larger (blue) and smaller (red) than 5.5. Middle: the same as in the top panel but zooming on the y-scale. Bottom. Cumulative annual rate computed for the considered catalog (red) and best fit exponential model (black line).

Figure 5. Seismic histories for four selected town in Central Asia considering both observed (red) and virtual (black) intensity data. The few available virtual points earlier than 1750 are not shown.

Figure 6 Top left: Seismic hazard in term of MSK64 intensity, estimated considering only the felt histories. Bottom left: seismic hazard estimated considering both felt histories and virtual intensities (i.e. computed by applying an intensity prediction equation to a seismic catalogue). Top right: the same as in the bottom left panel but the hazard is computed over a grid of points with resolution 0.1 degree. Bottom right: results from the GSHAP project

Figure 7 Probability of exceedance, for an exposure time of 50 years, obtained for the different localities and different intensities (VII, VIII and IX from top to bottom, respectively). The green circles (top and middle panels) indicate the epicenter of earthquakes with  $M > 7$ ; the green squares (bottom) those for  $M \geq 7.2$

Figure 8. Hazard curves (gray symbols and lines) computed for four major towns in Central Asia. The estimates from Nurmangambetov et al (1999) are also shown (black circles).

Figure 9. Top: Locations characterized by a probability of exceeding ( $p_0$ ) for  $I=VII$  in 50 years larger than 0.05. The color scale measures the difference between the probability of exceedance ( $p_{new}$ ) computed after adding an intensity  $I=VII$  to each seismic history and  $p_0$ , being the difference normalized to  $p_0$ . Middle: the same as in the top panel but

computing the probability for  $I=VIII$  for both the original data set and the one obtained after adding  $I=VIII$  to the seismic histories. Bottom: the same as in the middle panel but for  $I=IX$ .

Figure 10. Cumulative distribution functions (CDFs) relevant to the probability distributions shown in Figure 7. The curves for  $I=VII$ ,  $VIII$ , and  $IX$  are shown with different colors as indicated in the legend.

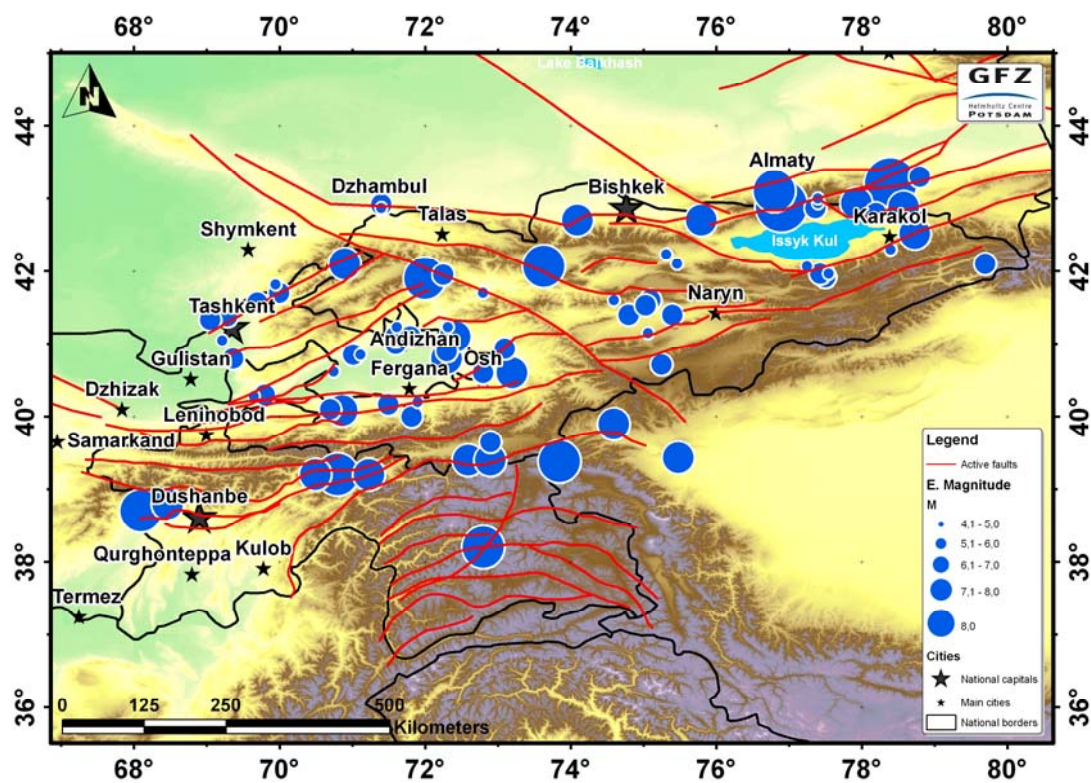
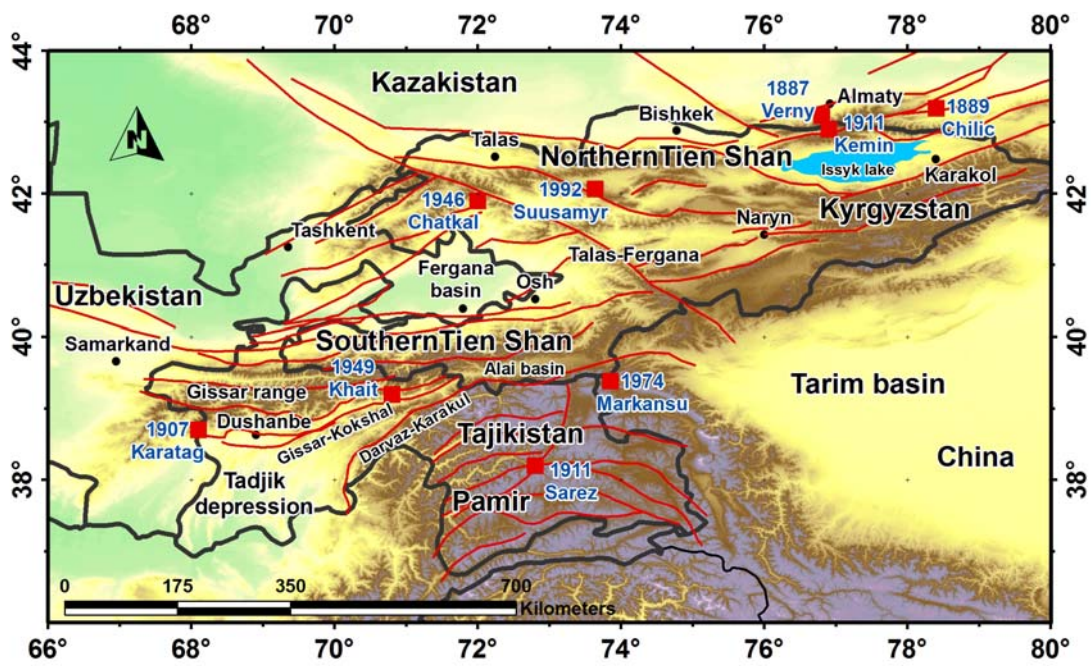


Figure 1



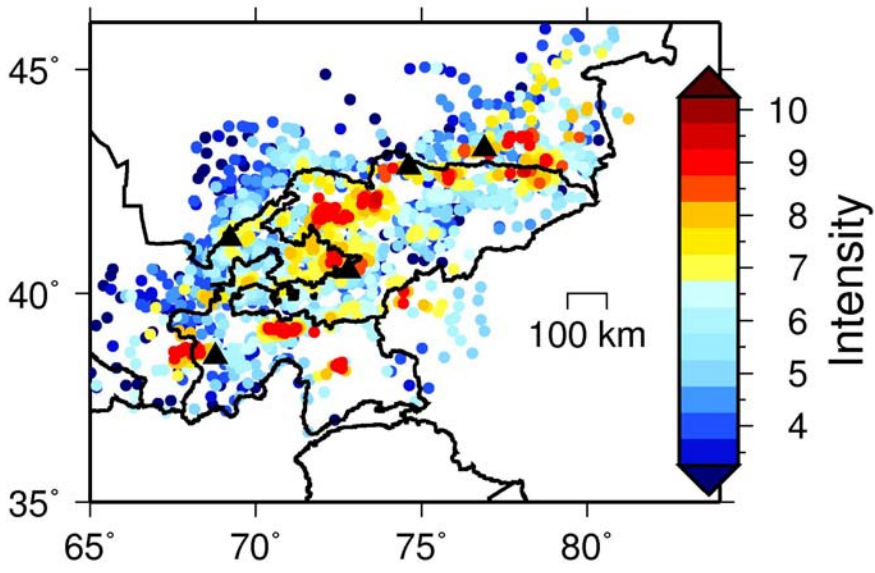
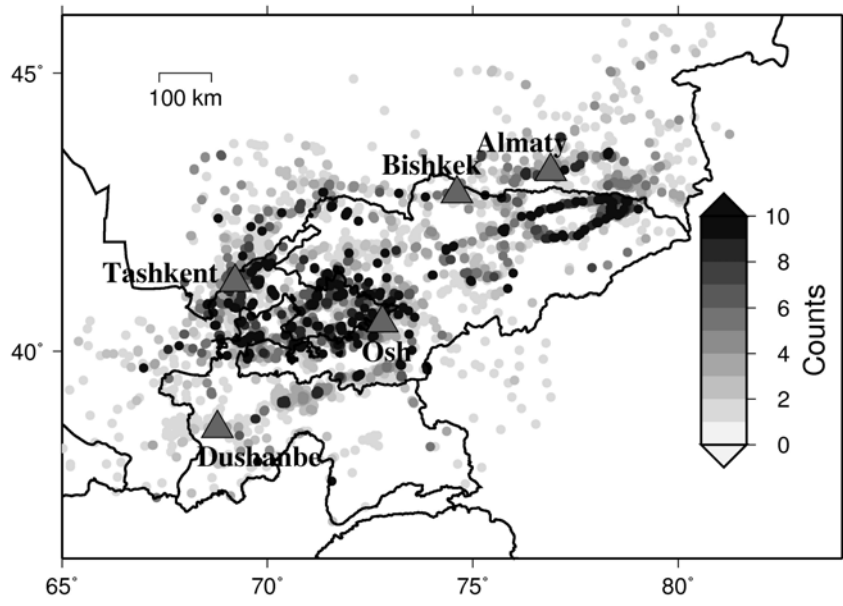
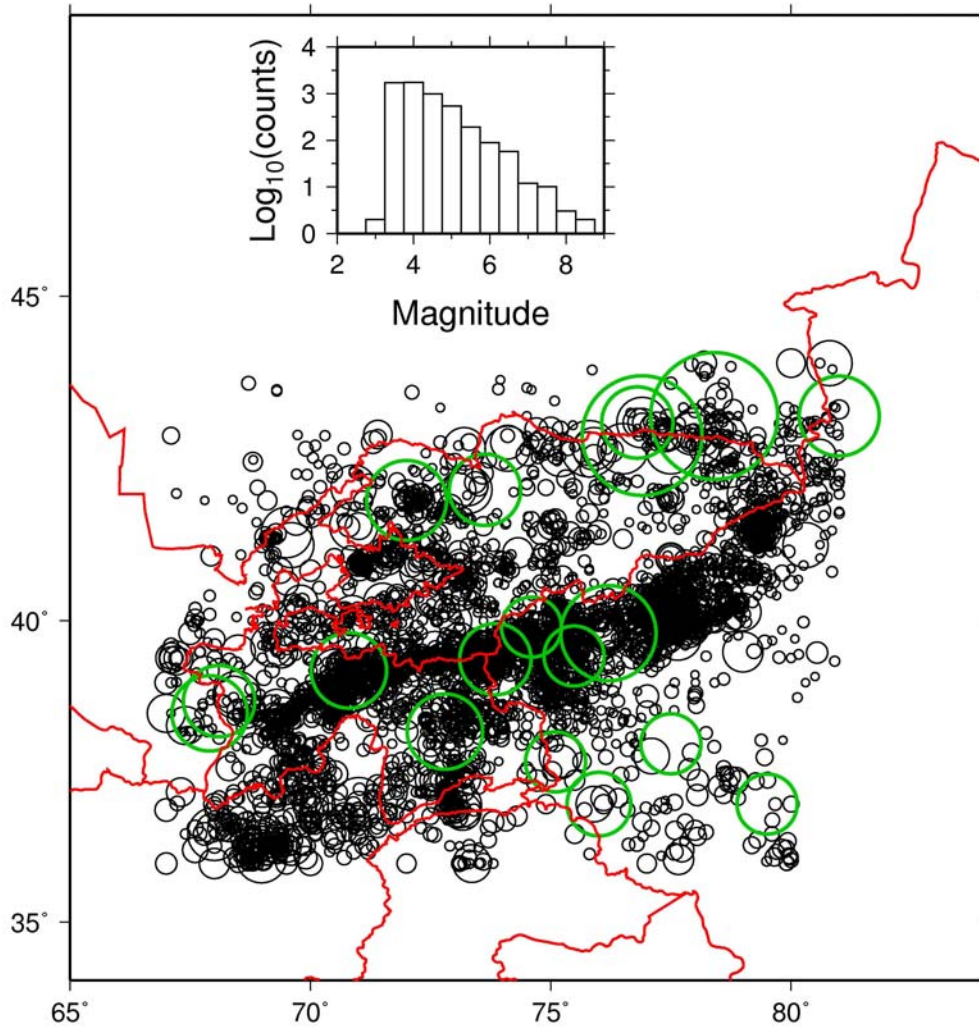


Figure 2



**Figure 3**

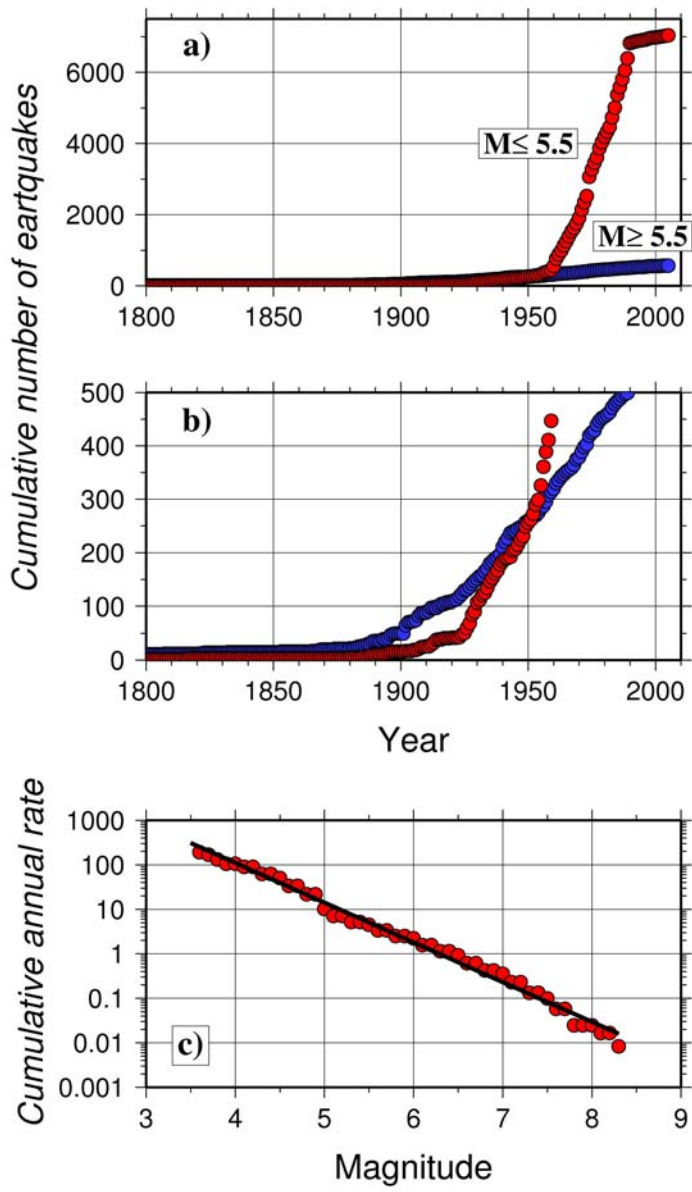


Figure 4

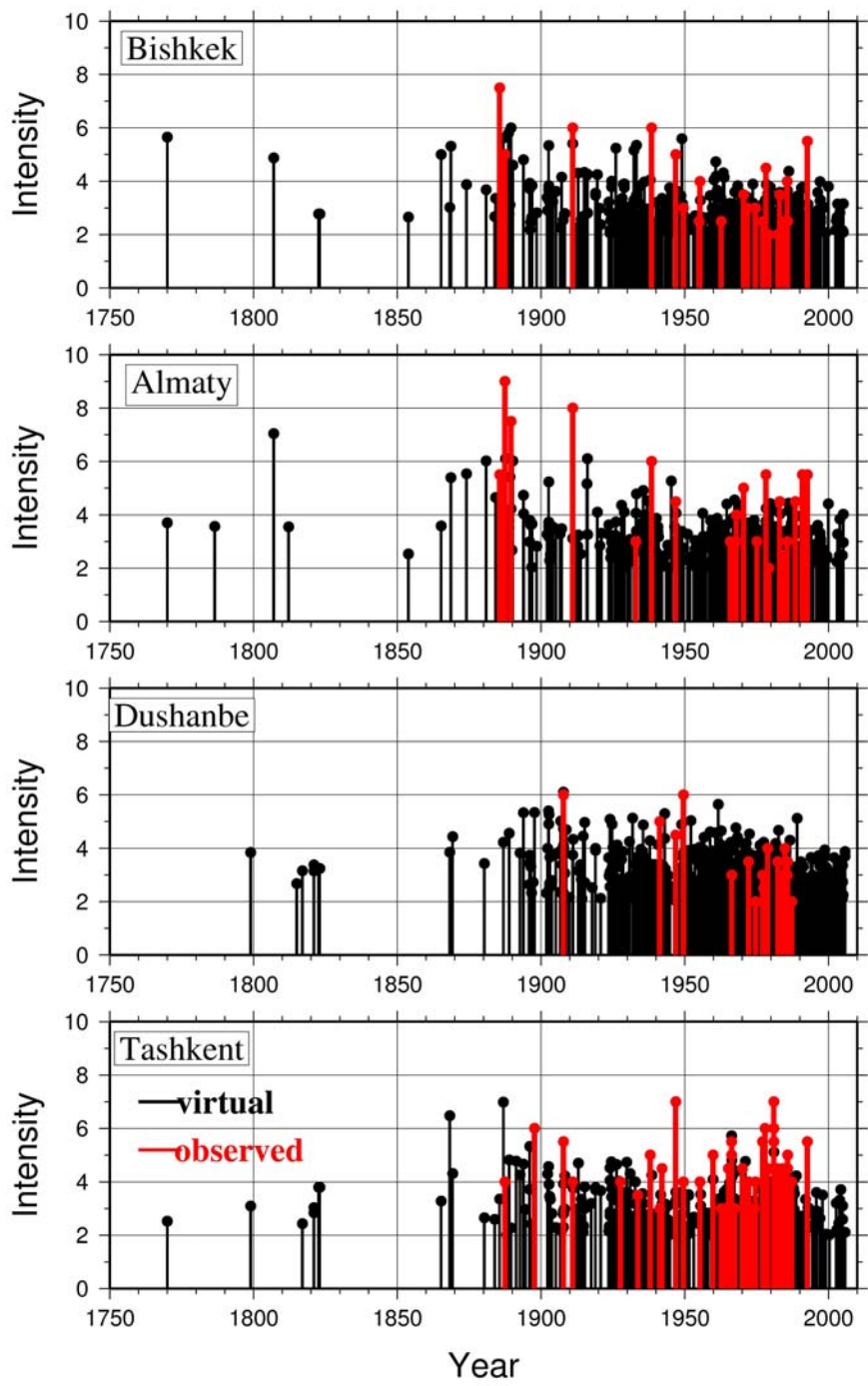
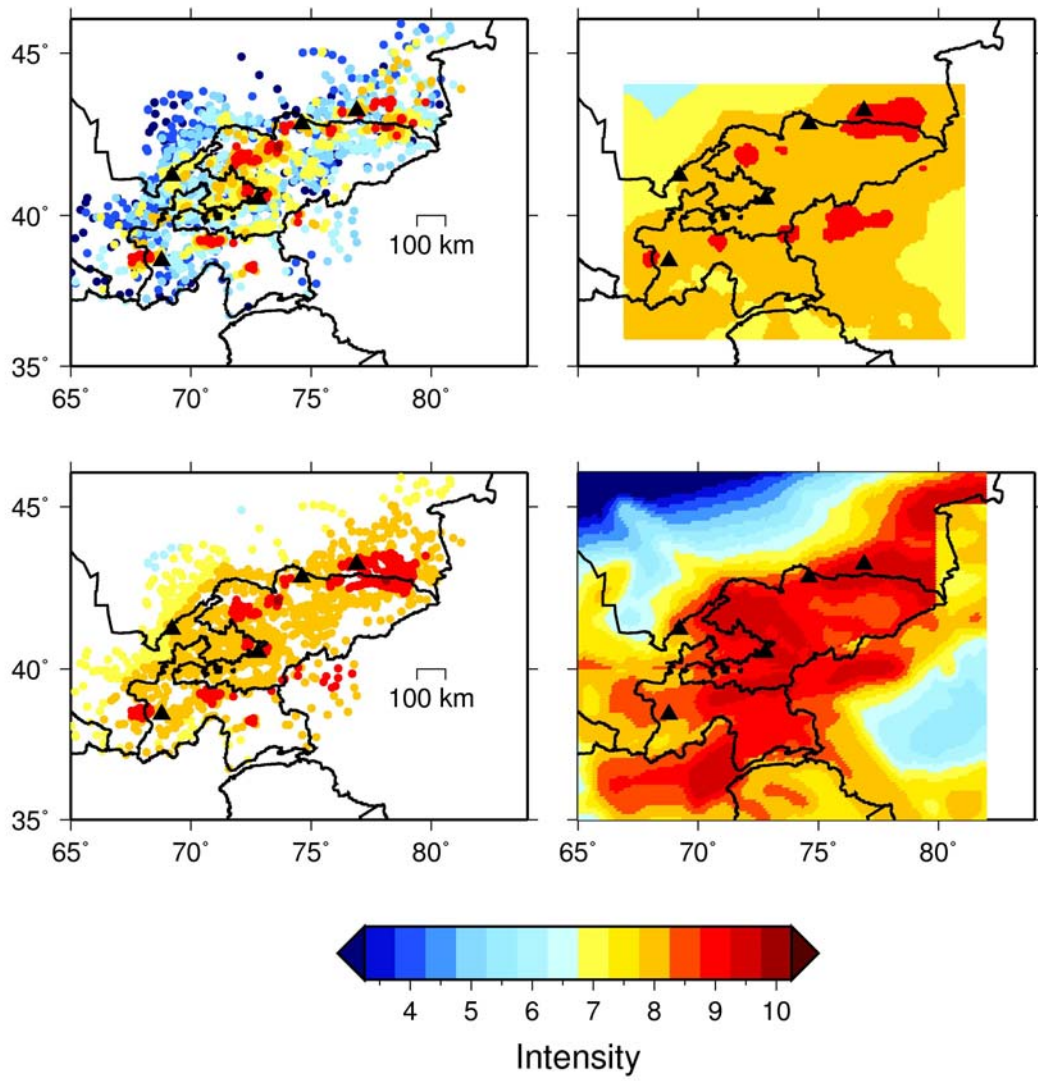


Figure 5



**Figure 6**



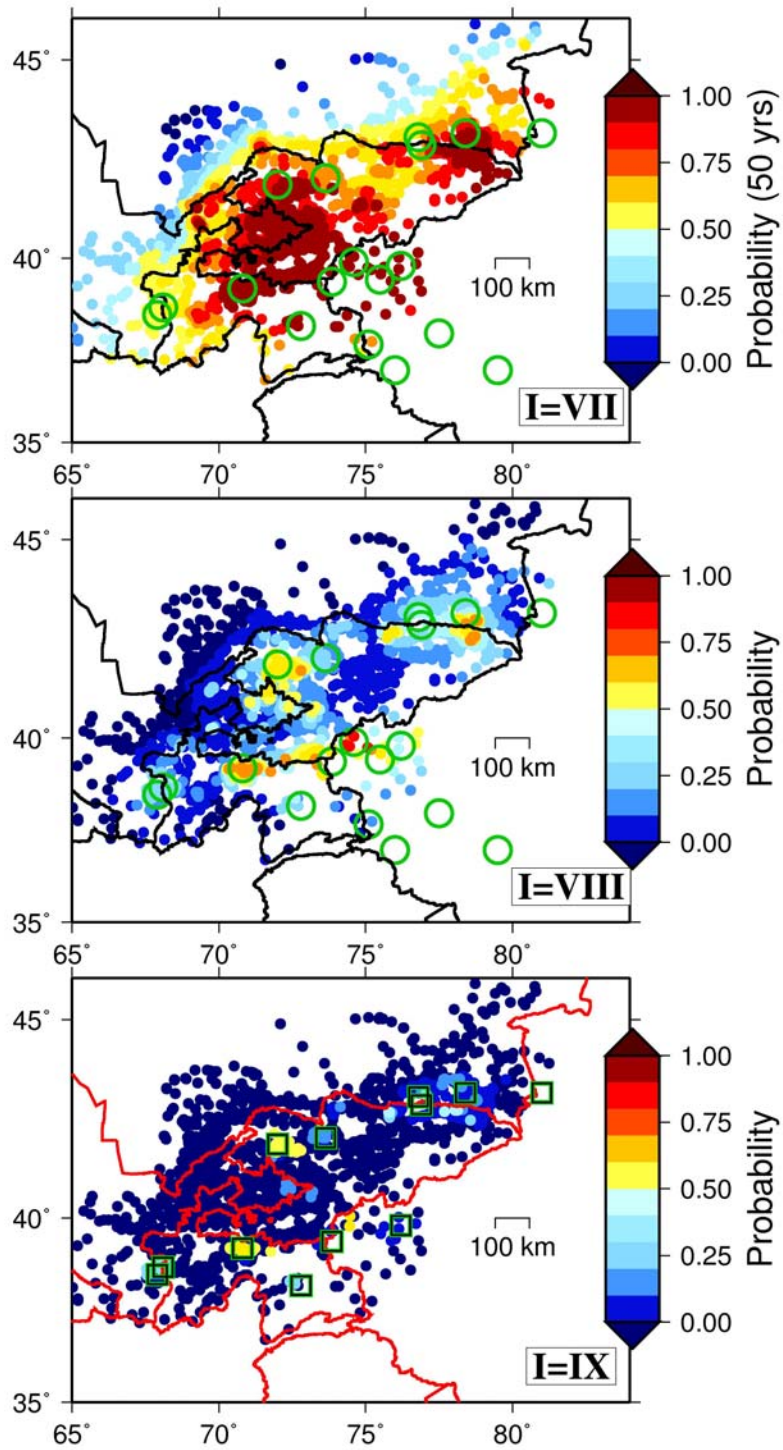


Figure 7

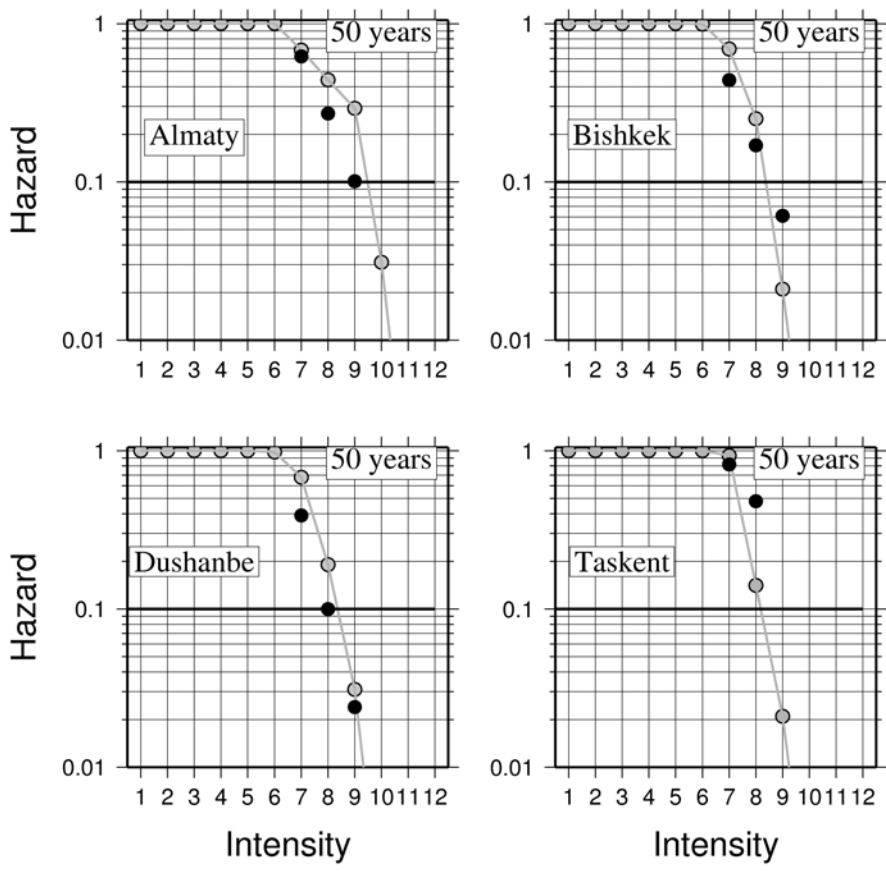
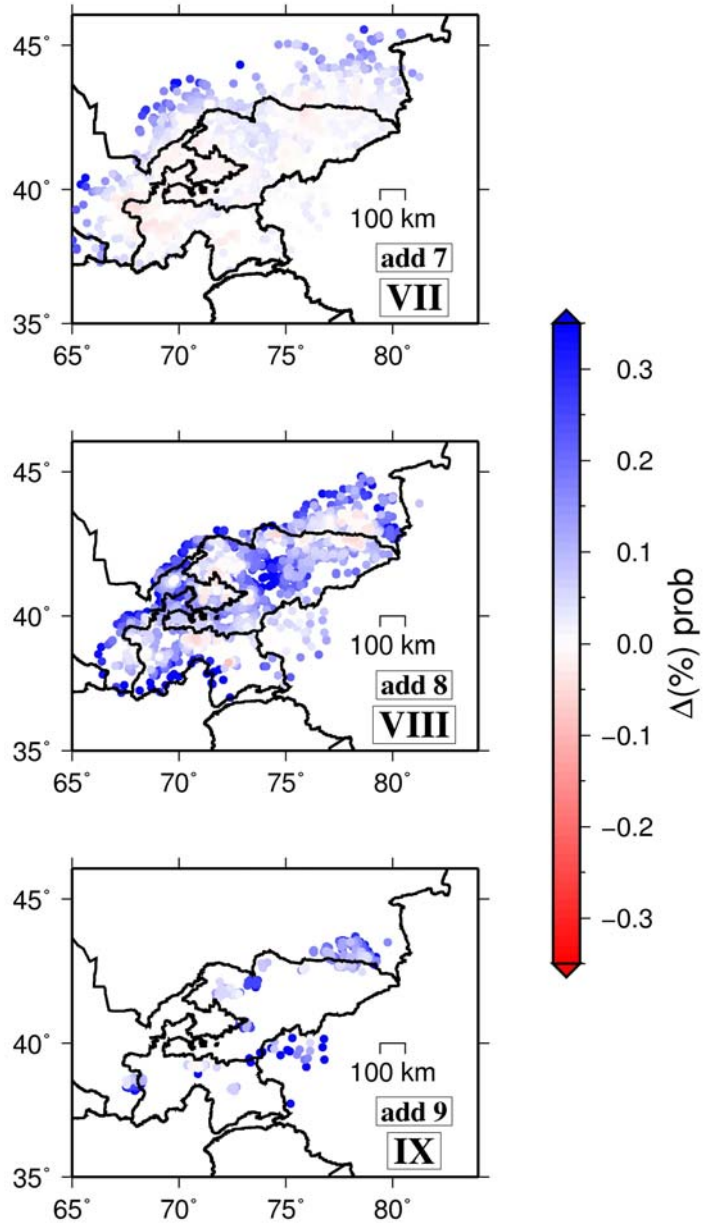


Figure 8



**Figure 9**



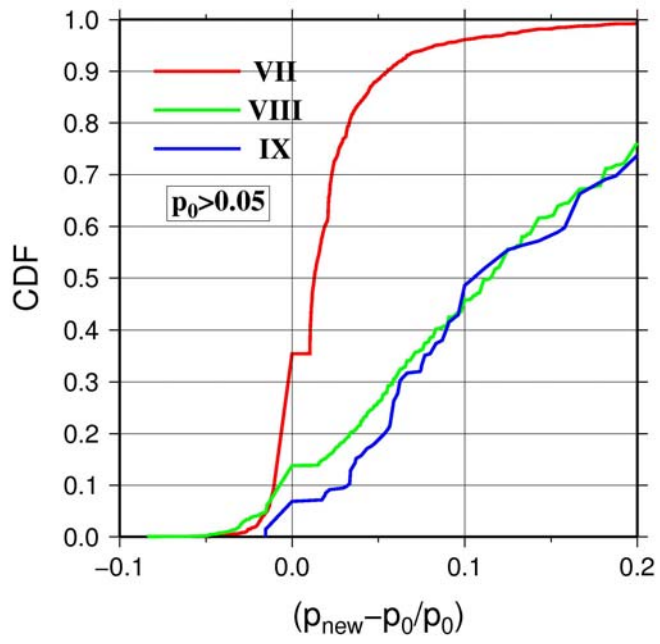


Figure 10